PASJ: Publ. Astron. Soc. Japan **64**, 115, 2012 October 25

GRB 100418A: a Long GRB without a Bright Supernova in a High-Metallicity Host Galaxy*

Yuu NIINO and Tetsuya HASHIMOTO
Division of Optical and IR Astronomy, National Astronomical Observatory of Japan, 2-21-1 Osawa, Mitaka, Tokyo 181-8588
yuu.niino@nao.ac.jp
Kentaro AOKI and Takashi HATTORI
Subaru Telescope, National Astronomical Observatory of Japan, 650 North A'ohoku Place, Hilo, HI 96720, USA
Kiyoto YABE†
Department of Astronomy, Kyoto University, Kitashirakawa-Oiwake-cho, Sakyo-ku, Kyoto 606-8502
and
Ken'ichi NOMOTO
Institute for the Physics and Mathematics of the Universe, The University of Tokyo, 5-1-5 Kashiwanoha, Kashiwa, Chiba 277-8583

(Received 2012 April 2; accepted 2012 May 6)

Abstract

We present results of a search for a supernova (SN) component associated with GRB 100418A at a redshift of 0.624. The field of GRB 100418A was observed with FOCAS on the Subaru 8.2 m telescope under a photometric condition (seeing 0.″3–0.″4) on 2010 May 14 (UT). The date corresponds to 25.6 days after the burst trigger (15.8 days in the restframe). We made imaging observations in the V, $R_{\rm c}$, and $I_{\rm c}$ bands, and two hours of spectrophotometric observations. We obtained a resolved host galaxy image that is elongated 1.″6 (= 11 kpc) from north to south. No point source was detected on the host galaxy. The time variation of the $R_{\rm c}$-band magnitude shows that the afterglow of GRB 100418A has faded to $R_{\rm c} \gtrsim 24$ without any SN-like rebrightening, when we compare our measurement to reports in GCN circulars. We could not identify any SN feature, such as broad emission-lines or bumps in our spectrum. Assuming the SN is fainter than the $3\,\sigma$ noise spectrum of our observation, we estimated the upper limit on the SN absolute magnitude to be $M_{I_{\rm c},\rm obs} > -17.2$ in the observer frame $I_{\rm c}$-band. This magnitude is comparable to the faintest type Ic SNe. We also estimated the host galaxy properties from the spectrum. The host galaxy of GRB 100418A is relatively massive ($\log M_\star/M_\odot = 9.54$) compared to typical long GRB host galaxies, and has $12 + \log({\rm O/H}) = 8.75$.

Key words: galaxies: abundances — gamma-ray burst: individual — stars: supernovae: individual

1. Introduction

Long gamma-ray bursts (GRBs) are now considered to be the death of massive stars (so called collapsar scenario). The most convincing observational evidence has been associations with supernovae (SNe). Some associations were spectroscopic, others were photometric. However, there is at least one long GRB, GRB 060614 (duration ~ 100 s, Della Valle et al. 2006; Fynbo et al. 2006), whose SN component was not detectable to very deep limits. GRB 060505 is also a $T_{90} > 2$ s burst without a detectable SN (Fynbo et al. 2006), although its duration of $T_{90} = 4$ s is close to the classical 2 s threshold that separates the long and short populations of GRBs.

Various progenitor models have been proposed to explain these events. Some have suggested they are short GRBs, which are considered to originate in mergers of a double compact object binary, with longer duration than typical short GRBs (Gehrels et al. 2006; Ofek et al. 2007; Levesque & Kewley 2007; Caito et al. 2009), while others point out similarities of these GRBs to other long bursts that originate from collapsars (McBreen et al. 2008; Thöne et al. 2008; Xu et al. 2009). The possibility of new populations that are different from long and short GRBs are also suggested for these GRBs (Gal-Yam et al. 2006; Lu et al. 2008). The sample of long GRBs with strong constraints on their SN components is still small, and it is still uncertain what impact the long GRBs without SNe have upon our understanding of the GRB populations.

Here, we present results of a search for a SN component associated with GRB 100418A. GRB 100418A was triggered on 2010 Aprili 18 at 20:10:08 UT (Marshall et al. 2010). The duration and the energetics of the prompt emission were $T_{90} = 8 \pm 2$ s and $E_{\rm iso} = (9.9^{+6.3}_{-3.4}) \times 10^{50}$ erg (Marshall et al. 2011). Follow-up spectroscopies of the optical transient (OT) detected emission-lines and absorption lines with a common redshift of 0.624 (Antonelli et al. 2010; Cucchiara & Fox 2010). Holland et al. (2010) pointed out that the light curve of GRB 100418A is similar to previous GRBs with SNe. Marshall and Holland (2010) reported a flattening of the optical light curve after 700 ks.

Throughout this paper, we assume fiducial cosmology with a Hubble constant of $71\,{\rm km\,s^{-1}\,Mpc^{-1}}$, $\Omega_\Lambda = 0.73$ and

* Based on data collected at Subaru Telescope, which is operated by the National Astronomical Observatory of Japan.

† Present address: Division of Optical and IR Astronomy, National Astronomical Observatory of Japan, 2-21-1 Osawa, Mitaka, Tokyo 181-8588.

Table 1. Observation log.

UT date midpoint of exposures	Time after the burst (d)	Filter	Exposure time (s)
14.50969	25.62765	R_c	120
14.51178	25.62974	I_c	120
14.51388	25.63184	V	120
14.51705	25.63501	(Unbinned) R_c	120 × 2
14.56639	25.68435	300R+O58	1200 × 3
14.57130	25.68926	300B	1200 × 3

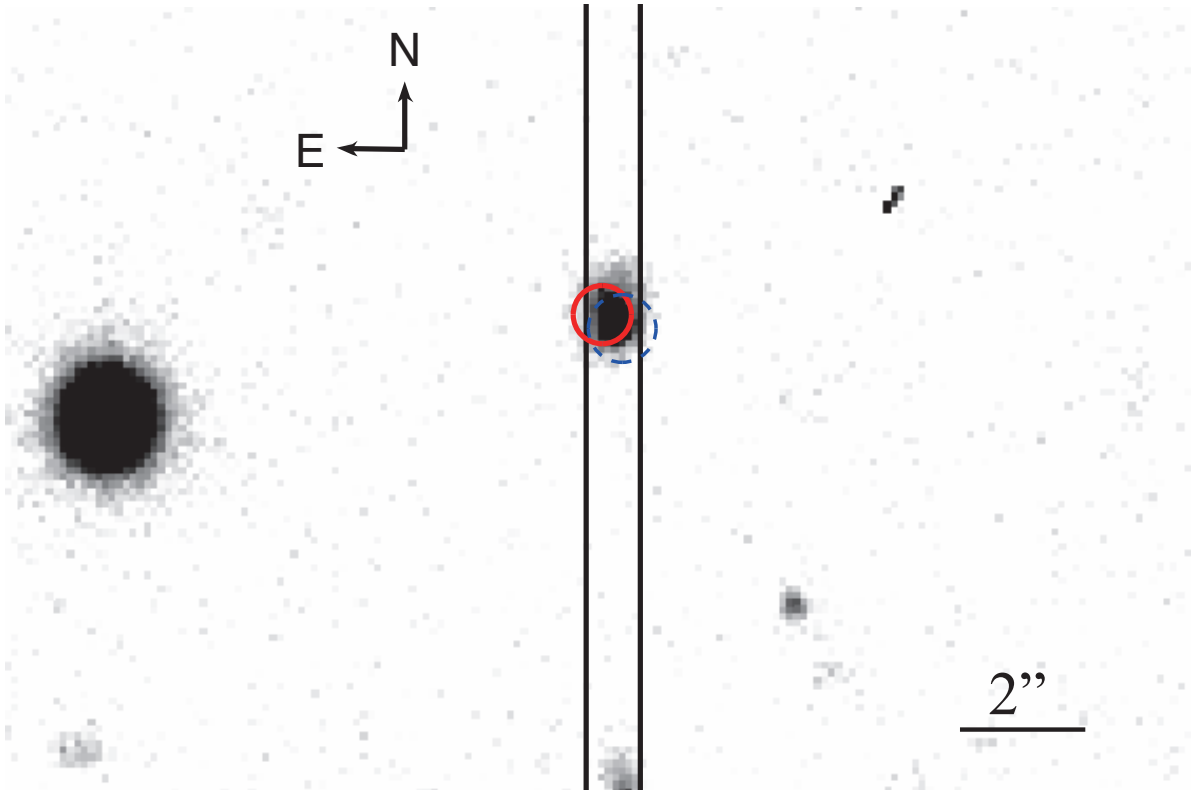

Fig. 1. R_c-band image of the GRB 100418A host galaxy (unbinned, 0.″103/pixel). The circles indicate localizations of the optical counterpart in earlier epoch observations by UVOT (Marshall et al. 2011, red solid) and GROND (Filgas et al. 2010, blue dashed), respectively. The slit position for our spectroscopy is shown with vertical lines. A colored version of the figure is available in an online journal.

$\Omega_m = 0.27$. The angular scale is thus 6.8 kpc arcsec^{-1}. We use the AB magnitude system unless otherwise stated.

2. Observations and Reductions

We observed the field of GRB 100418A with FOCAS (Kashikawa et al. 2002) on Subaru Telescope (Iye et al. 2004) under a photometric condition (seeing 0.″3–0.″4) on 2010 May 14 (UT). We started imaging observations in the V, R_c, and I_c bands at 12:13 UT, and spectroscopic observations followed. The log of the observations is tabulated in table 1. We acquired a single exposure of 120 s in each of the V, R_c, and I_c bands with 2 × 2 binning, which yields a pixel scale of 0.″206/pixel. Unbinned R_c-band images were also taken with 0.″103/pixel.

Spectroscopy was performed with a 0.″8 width slit and 3 pixels binned along the spatial direction, and two different settings of grisms and an order-cut filter. One setting covered a wavelength range between 5800 Å and 10200 Å with the R300 grism and the O58 order-cut filter, and the other covered between 3900 Å and 8300 Å with the B300 grism and no order-cut filter. The total integration time was 1 hr (1200 s × 3) for each of the settings. We used an atmospheric dispersion corrector, and set the slit position angle to 0.°0, i.e., north-south. The spectral resolution was ∼ 11 Å in both settings.

The data were reduced using IRAF[1] for the procedures

[1] IRAF is distributed by the National Optical Astronomy Observatory, which is operated by the Association of Universities for Research in Astronomy (AURA), Inc., under cooperative agreement with the National Science Foundation.

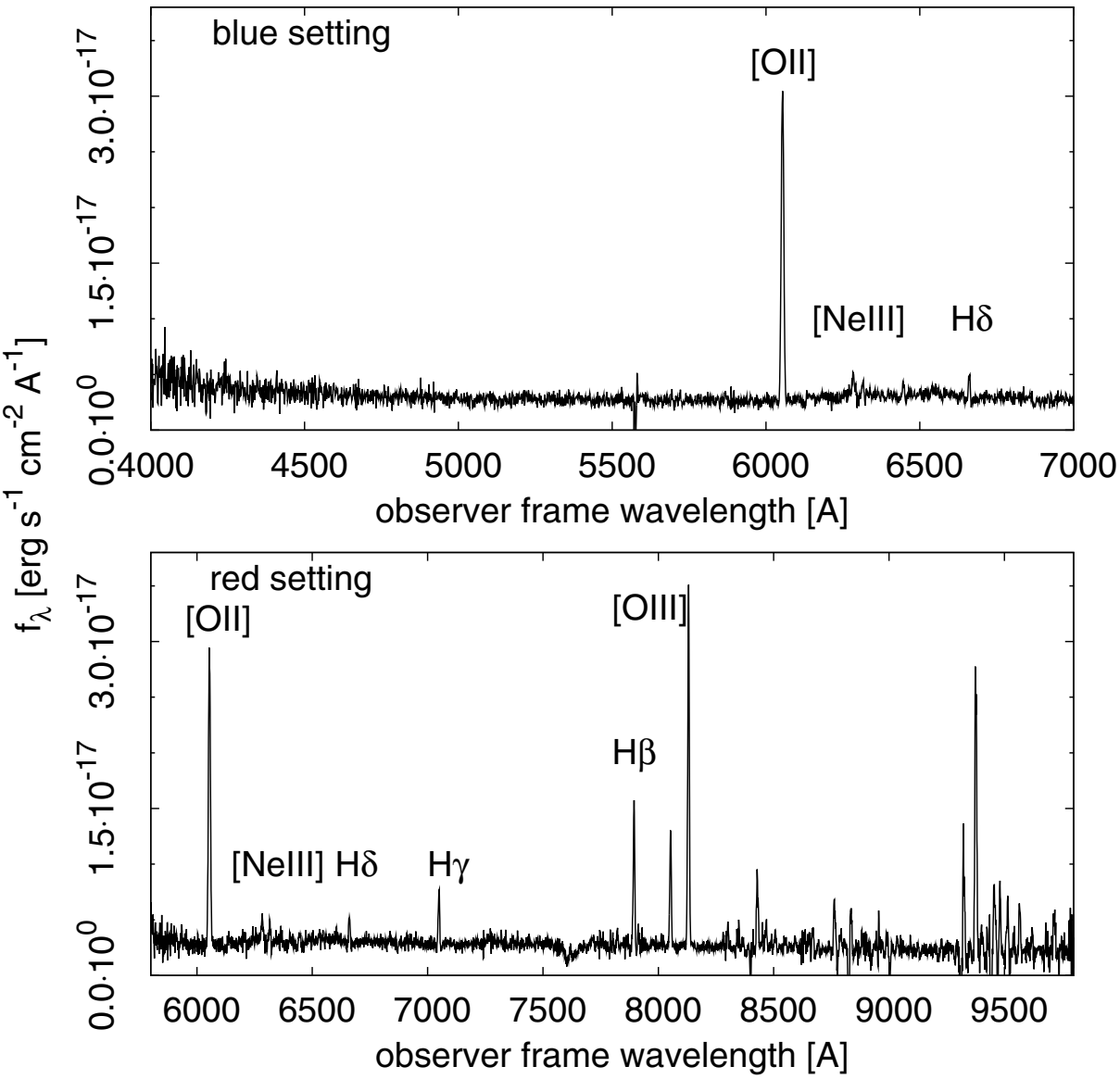

Fig. 2. Observed spectrum of the GRB 100418A host galaxy.

of bias subtraction and flat-fielding. The spectra were wavelength calibrated, and sky subtracted. A wavelength calibration was performed using night-sky emission lines for the red setting and ThAr arc lines for the blue setting; the rms wavelength calibration error is 0.2–0.3 Å. A sensitivity calibration was performed as a function of the wavelength by using the spectrum of Feige 34 observed with a 2″ width slit. For imaging data, a flux calibration was carried out by observing the standard star PG 1505−027 field (Stetson 2000) on the same night.

An R_c-band image of 0.″103/pixel is shown in figure 1, and the observed spectra are shown in figure 2. These spectra were made by summing 2.″5 along the slit in order to include all galaxy light. We found strong emission lines, such as [O II], Hγ, Hβ, [O III], which are redshifted by 0.624 consistently to previous reports (Antonelli et al. 2010; Cucchiara & Fox 2010).

3. Constraints on the Associated Supernova

3.1. Time Variation of Broad-Band Magnitudes

We detected the host galaxy, which has been catalogued in Sloan Digital Sky Survey (SDSS) as $g = 22.89 \pm 0.17$, $r = 22.41 \pm 0.16$, $i = 21.94 \pm 0.17$ (Malesani 2010). The host galaxy is resolved in our images. It elongates 1.″6 (= 11 kpc) from north to south. A bright spot locates at the southern tip of the galaxy. The size of this bright spot is 0.″47 FWHM, while the stars' FWHMs are 0.″32. The spot is clearly extended, and not a point source. Aperture photometry of the host galaxy gives $V = 22.61 \pm 0.06$, $R_c = 22.10 \pm 0.03$, and $I_c = 21.80 \pm 0.05$. Our R_c-band magnitude is consistent with that reported by Rumyantsev and Pozanenko (2010a), $R = 22.06 \pm 0.06$ at 26.0 d after the burst.

The time variation of the R-band magnitude between 5 and

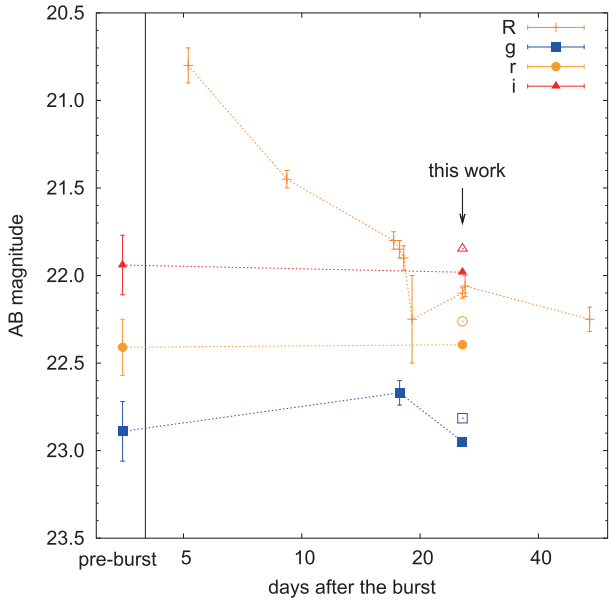

Fig. 3. Time variation of broad-band photometry in GRB 100418A optical follow up observations (afterglow, host galaxy, and potential supernova). The open symbols for the g, r, and i-band indicates the correction for possible slit loss. We collected data points other than our observation from the GCN circulars (Bikmaev et al. 2010a, 2010b; Malesani 2010; Perley et al. 2010; Rumyantsev & Pozanenko 2010a, 2010b; Volnova et al. 2010). A colored version of the figure is available in an online journal.

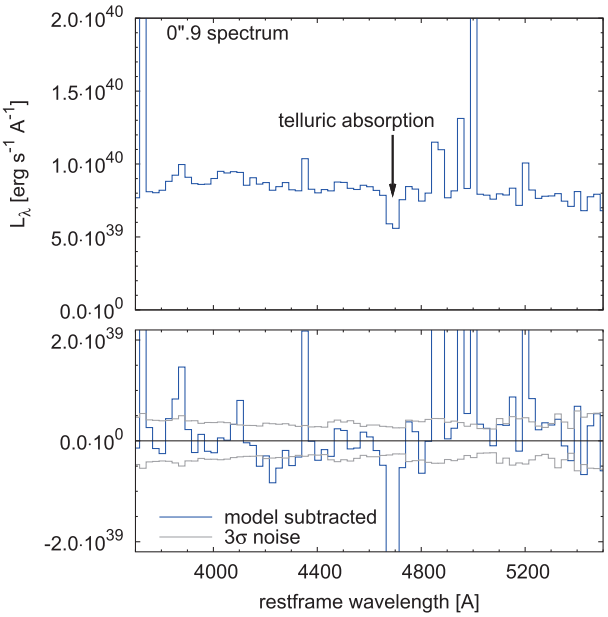

Fig. 4. Top panel: the observed spectra at the brightest 0.″9 of the host galaxy. Bottom panel: the model subtracted 0.″9 spectrum (thick histogram) compared to 3 σ noise spectrum (thin histogram).

54 d after the burst is shown in figure 3, together with the g, r, and i-band magnitudes in the SDSS catalog (pre-burst) and those at 25.6 d after the burst. The g, r, and i-band magnitudes at 25.6 d ($g = 22.95$, $r = 22.40$, and $i = 21.98$ with photometric errors < 0.01 mag) were calculated from our spectrum of the host galaxy following equation (3) in Smith et al. (2002). The R-band time variation shows a smooth decline of afterglow, expect for one datapoint with a large error bar at 19.1 d after the burst. SN-like rebrightening is not recognizable.

The g, r, and i-band magnitudes calculated from the FOCAS spectrum are consistent with SDSS pre-burst magnitudes. However, it should be noted that the R_c-band magnitude is 0.13 mag fainter when calculated from the spectra than that in aperture photometry, possibly due to a loss of light at the slit. The spectrum is still consistent with the pre-burst magnitudes within the SDSS photometric error when a 0.13 mag slit loss correction is applied; however it is systematically brighter in all of the three bands. Rumyantsev and Pozanenko (2010b) reported $R = 22.25 \pm 0.07$ at 54.0 d after the burst, which is 0.15 mag fainter than our photometry at 25.6 d. Thus, it is possible that our image and spectrum contain a small fraction of afterglow (and potential supernova) light, although no point source has been detected on the host galaxy, as described above. We compared the calculated i-band magnitude with the SDSS photometry after the slit loss correction, and obtain upper limit on the OT, $M_{i,\mathrm{obs}} > -19.1$ (95% limit, afterglow plus potential supernova). Note that observer frame i-band covers $\sim$4200–5300 Å in the restframe.

3.2. *Bright Spot Spectrum*

The OT position reported by Filgas, Klose, and Greiner (2010) and Marshall et al. (2011) corresponds to the brightest spot of the host galaxy (figure 1). To search for SN features in our spectra, we extracted the spectrum of the brightest part (0.″9) of the host galaxy, which corresponds to the error circles of the OT localization. The 0.″9 spectrum is shown in the top panel of figure 4. The spectrum is 30 pixel binned along the wavelength (= 40.2–40.5 Å in the observerframe), in order to increase the signal-to-noise ratio (S/N). The 0.″9 spectrum shows no SN feature like broad emission-lines or bumps. We subtracted a stellar spectral energy distribution (SED) model of the host galaxy (see section 4) from the 0.″9 spectrum. Because the SED model was fitted to the whole galaxy spectrum, it was scaled 75% to match the 0.″9 spectrum. The subtracted spectrum is shown in the bottom panel of figure 4, together with the 3 σ noise spectrum. Although it is possible that the afterglow and the SN affect the SED model, and our spectra suffers from residulals of the OH sky lines, showing larger fluctuation than expected from the noise level, it shows no broad feature ($\gtrsim$ 200 Å) above the 3 σ noise. Thus, we estimated upper limit of the SN light while assuming it is fainter than the 3 σ noise spectrum.

Spectrum of a SN (L_λ) peaks at 5000–5500 Å in its restframe, and hence the V-band magnitude is popularly used to discuss the SN brightness at lower redshifts. However, our spectrum suffers from strong OH sky lines in the higher-end of the restframe V-band ($\gtrsim$ 9000 Å in observer frame, see figure 2), and S/N is poor. Instead, we calculated the constraint on the SN component in the observer frame I_c-band, which also covers the restframe 5000–5500 Å, and consider it is comparable to the V-band magnitudes of other SNe at lower redshfits. We note that the line-of-sight extinction

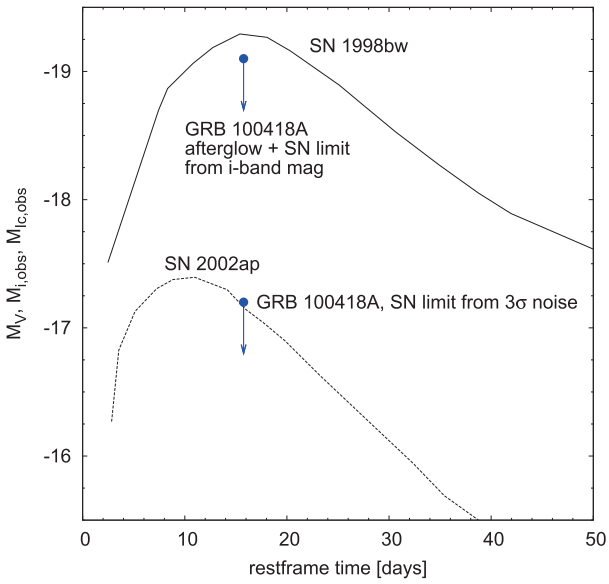

Fig. 5. Constraint on the SN component associated with GRB 100418A. The observer frame i-band limit from broad-band photometry (afterglow + SN), and observer frame I_c-band limit from the $3\,\sigma$ noise spectrum (SN only) are compared to V-band light curves of broad-lined type Ic SNe in the literature (Galama et al. 1998; Mazzali et al. 2002).

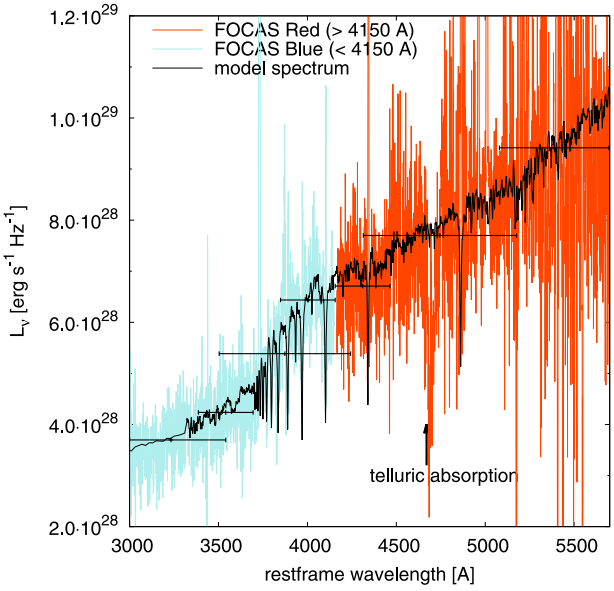

Fig. 6. Best-fit SED model (thick black line) is compared to the observed spectrum (thin light-colored line), and corresponding band magnitudes to which the fitting is performed. The observed spectra is taken from the blue setting spectroscopy below 4150 Å, and from the red setting above (light-blue and orange in colored version). A colored version of the figure is available in an online journal.

of GRB 100418A within its host galaxy is small, $E(B-V) = 0.056$, based on the X-ray afterglow spectrum (Marshall et al. 2011). The $3\,\sigma$ noise spectrum is equivalent to the absolute magnitude $M_{I_c,\mathrm{obs}} = -17.2$ after being corrected for extinction (figure 5).

4. Properties of the Host Galaxy

We perform an SED fitting using the *SEDfit* software package (Sawicki 2012; Yabe et al. 2009), which utilizes population synthesis models by Bruzual and Charlot (2003) and an extinction law by Calzetti et al. (2000). After correcting for the Milky Way extinction $E(B-V) = 0.072$ (Schlegel et al. 1998), the spectrum was converted to magnitudes in the 8 bands shown in figure 6, collected from both of the blue and red settings of the spectroscopy, while avoiding a wavelength range where the detector sensitivity is poor and/or the OH sky line is strong. The stellar metallicity is assumed to be $Z_\odot$ for consistency with the emission-line diagnostic discussed below. However, we note that the results with the $0.24\,Z_\odot$ model are not significantly different. We examined seven cases of star-formation history: simple stellar population (SSP), constant star formation, and exponentially decaying star formation with $\tau = 10^{-3}$, 10^{-2}, 0.1, 1, and 10 Gyr, among which SSP provides the best fit.

We find that the SED model reproduces our spectrum with the parameters listed in table 2. [The initial mass function (IMF) of Salpeter (1955) is assumed.] The best-fitting SED model is shown in figure 6. As discussed in subsection 3.1, our spectrum may be contaminated by GRB afterglow. We also tried an SED fitting by subtracting an afterglow model from our spectrum; however, the results are similar to the case without any afterglow subtraction. The assumed afterglow model is that the late time spectral index of GRB 100418A afterglow $\beta = 1.15$ (Marshall et al. 2011), and the flux in the R-band is $F_\nu = 6.8 \times 10^{-30}\,\mathrm{erg\,s^{-1}\,cm^{-2}\,Hz^{-1}}$, which is derived from the difference between the R-band magnitudes at 25.6 d and 54.0 d (see figure 3). The results of the afterglow subtracted SED fitting is included in the errors given in table 2.

Table 2. Results of SED fitting.

$\log M_\star$	Age [Gyr]	$E(B-V)$	χ^2
$9.54^{+0.28}_{-0.03}$	7.1–8.1	$0.38^{+0.06}_{-0.09}$	13.1

We measured the metallicity of the host galaxy using emission-line diagnostics. We performed a linear continuum plus single Gaussian fit to each line, after subtracting the best-fit SED model (figure 6) from the observed spectrum, to minimize the effect of stellar absorption features, such as Balmer absorption lines. The best-fit SED was obtained assuming stellar metallicity, $Z_\odot$, but using the SED model with $0.2\,Z_\odot$ did not make any significant difference. The resulting line fluxes are listed in table 3. The Hβ/Hγ ratio is consistent to zero extinction; thus, we assume there is no reddening on emission lines, except for that in the Milky Way.

We used the R_{23} method described in Kobulnicky and Kewley (2004), which gave two solutions of possible metallicity (upper and lower branch):

$$12 + \log(\mathrm{O/H})_{\mathrm{upper}} = 8.75, \quad (1)$$

$$12 + \log(\mathrm{O/H})_{\mathrm{lower}} = 7.94. \quad (2)$$

Nagao, Maiolino, and Marconi (2006) found that the [Ne III]3869/[O II]3727 line flux ratio correlates with

Table 3. Emission-line fluxes of the GRB 100418A host galaxy (10^{-17} erg s^{-1} cm^{-2}).

[O II]3727	[Ne III]3869	Hγ	Hβ	[O III]4959	[O III]5007	log O_{32}	log R_{23}
25.1 ± 0.2	1.49 ± 0.16	4.30 ± 0.10	9.10 ± 0.18	7.48 ± 0.12	22.4 ± 0.2	0.0757	0.781

the metallicity, and thus can be used as an indicator to separate these two solutions. They showed that galaxies with $12 + \log(\mathrm{O/H}) \geq 8.65$ have log [Ne III]3869/[O II]3727 < -1.1, while galaxies with $12 + \log(\mathrm{O/H}) < 8.05$ have log [Ne III]3869/[O II]3727 > -0.79. The host galaxy of GRB 100418A has log [Ne III]3869/[O II]3727 $= -1.23$, which suggests that the upper-branch solution is the case.

There are several emission-line diagnostics proposed to measure metallicity, and their results are not always consistent with each other (e.g., Kewley & Ellison 2008). We note that the metallicities discussed in Nagao, Maiolino, and Marconi (2006) is measuered using the Tremonti et al. (2004) method for high-metallicity galaxies, and the electron-temperature method (Izotov et al. 2006) for low-metallicity galaxies. However, the difference between the results of the Kobulnicky and Kewley (2004) method and that of the Tremonti et al. (2004) method is small in the high-metallicity range, and the Kobulnicky and Kewley (2004) method tends to result in a higher-metallicity in the low-metallicity range compared to other methods (Kewley & Ellison 2008). Hence, the difference between the metallicity calibration we used and that used in Nagao, Maiolino, and Marconi (2006) would not confuse the separation of the two branches.

We also estimated the star-formation rate (SFR) of the host galaxy from the emission line flux. Following the Hβ–SFR relation used in Savaglio, Glazebrook, and Le Borgne (2009) in which the IMF of Baldry and Glazebrook (2003) is assumed, SFR of the host galaxy is $1.88\,M_\odot\,\mathrm{yr}^{-1}$, or $3.38\,M_\odot\,\mathrm{yr}^{-1}$ when re-scaled with the Salpeter IMF, which is consistent with the stellar mass measured in the SED fitting. The specific SFR $0.98\,\mathrm{Gyr}^{-1}$ is typical of long GRB host galaxies with $\log M_\star/M_\odot \sim 9.5$ (Savaglio et al. 2009).

5. Discussion

We have presented the results of the search for SN component associated with GRB 100418A, with FOCAS on the Subaru telescope. Both imaging and spectroscopic observations show no evidence of SN. A comparison of our i-band magnitude to pre-burst data in the SDSS catalog puts an upper limit on the afterglow plus the SN luminosity, $M_{i,\mathrm{obs}} > -19.1$. Our spectrum shows no SN feature above the noise level. Assuming that the SN is fainter than the noise level, we estimate the upper limit on the SN to be $M_{I_\mathrm{c},\mathrm{obs}} > -17.2$ (4400–5500 Å in the restframe). This limit is about 4 magnitudes brighter compared to the cases of GRB 060505 and GRB 060614 at $z \sim 0.1$, due to the higher redshift of GRB 100418A ($z = 0.624$) and the brightness of the host galaxy. However, it is still comparable to the faintest type Ic SNe, including SN 2002ap, which is the faintest broad-lined type Ic SN ever observed (Drout et al. 2011; Richardson 2009; Mazzali et al. 2002).

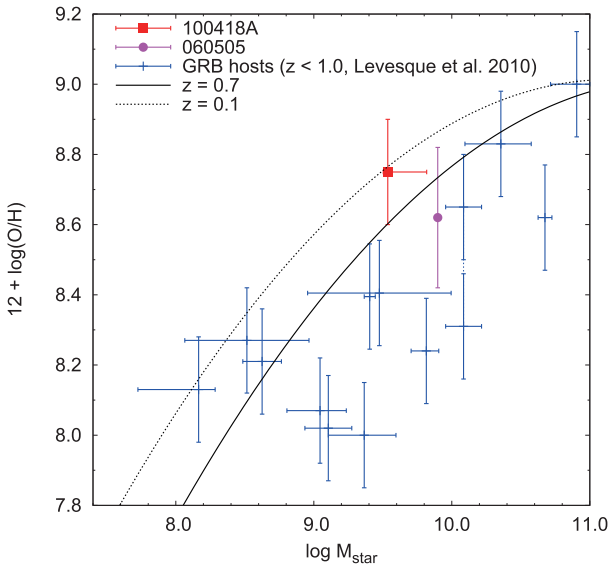

Fig. 7. Stellar mass and metallicity of the host galaxy of GRB 100418A (red square). The stellar mass and metallicity of the host galaxy of GRB 060505 (Levesque & Kewley 2007; Thöne et al. 2008, magenta circle), and other GRB host galaxies at $z < 1.0$ (Levesque et al. 2010, blue crosses) are plotted together. The mass–metallicity relation of field galaxies at redshfits of 0.1 and 0.7 is shown for a comparison (Savaglio et al. 2005). All metallicities were calibrated with the method of Kobulnicky and Kewley (2004), and the stellar masses were re-scaled with the Salpeter IMF. A colored version of the figure is available in an online journal.

We have also estimated the properties of the host galaxy of GRB 100418A. The results of the SED fitting and the emission-line diagnostic show that the host galaxy has a larger stellar mass and higher-metallicity than the majority of long GRB host galaxies at $z < 1.0$ (figure 7). It is notable that among three long GRBs with a significant limit on their SN component, two bursts occurred in galaxies with $12 + \log(\mathrm{O/H}) > 8.6$ (GRB 060505 and GRB 100418A). The other one burst, GRB 060614, occurred in a very faint galaxy (Gal-Yam et al. 2006), and the metallicity of the host galaxy was not measured.

A. de Ugarte Postigo et al. (in preparation) reported a possible detection of the SN component of GRB 100418A at 28 d after the burst, which is faint, and agrees with our upper limit. The possible SN association suggests that GRB 100418A maybe originate from a collapsar. If their possible detection is a real event, the SN associated with GRB 100418A is the faintest SN associated with a GRB (Richardson 2009), except for another possibly detected SN associated with GRB 101225A (Thöne et al. 2011, but see also Campana et al. 2011).

The specific SFR of the host galaxy of GRB 100418A is comparable to other long GRB host galaxies, suggesting

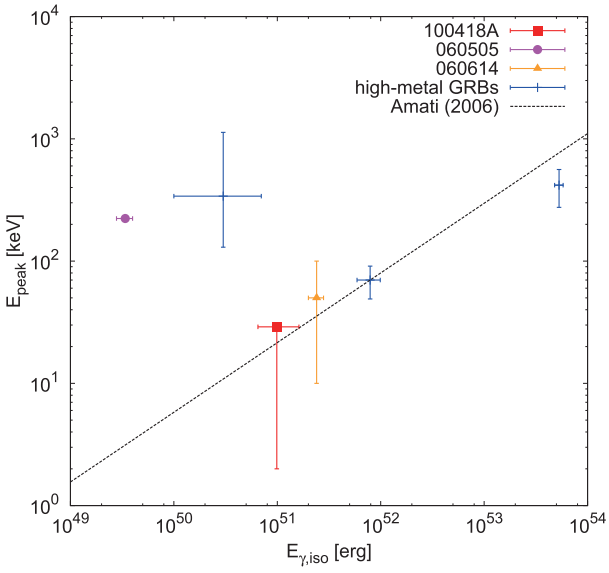

Fig. 8. $E_{\rm peak}$ and $E_{\gamma,\rm iso}$ of long GRBs without SNe and long GRBs in high-metallicity host galaxies at $z < 1.0$. GRB 100418A, 060505, and 060614 are shown with filled square (red), circle (magenta), and triangle (orange), respectively. Other bursts are shown with crosses (blue). The $E_{\rm peak}$ and the $E_{\gamma,\rm iso}$ of GRB 100418A is taken from Marshall et al. (2011). We take data for the rest of the bursts from Zhang et al. (2009) and Amati et al. (2007). The relation between $E_{\rm peak}$ and $E_{\gamma,\rm iso}$ of long GRBs presented in Amati (2006) is plotted together. A colored version of the figure is available in an online journal.

a collapsar origin of this burst, while short GRBs occur in galaxies with lower specific SFR than host galaxies of long bursts (Berger 2009). However, it should be noted that a short GRB (XRF) 050416 occurred in a galaxy with a similar $M_\star$ and SFR to the host galaxy of GRB 100418A (Soderberg et al. 2007).

In figure 8, we show the spectral peak and the isotropic equivalent gamma-ray energy of GRB 100418A (Marshall et al. 2011) together with those of GRB 060505, 060614 and other GRBs at $z < 1.0$ whose host galaxies are metal rich. GRB 100418A and 060614 agree with the $E_{\rm peak}$–$E_{\gamma,\rm iso}$ relation of long GRBs by Amati (2006), while GRB 060505 is in upper-left of the relation where most short bursts reside (Amati et al. 2007). A caveat on this plot is that the $E_{\rm peak}$ of GRB 100418A is calculated in Marshall et al. (2011) using a relation between the photon index in *Swift* Burst Alert Telescope and $E_{\rm peak}$ (Sakamoto et al. 2009), which has not been tested against short GRBs. Thus, some observational features suggest that GRB 100418A originates from a collapsar; however, none of them are conclusive.

The sample of long GRBs without bright SNe and long GRBs in high-metallicity galaxies is still very small, and it is difficult to draw any robust conclusions concerning their nature. However, the localization of a long GRB without a bright SN in a high-metallicity galaxy suggests some interesting possibilities. If long GRBs without observable SNe originate from collapsars similarly to GRBs with hypernove, many occur in low-metallicity galaxies. The possible high-metallicity environments of long GRBs without SN features suggest environmental effect on explosion scenario in which a collapsar produces no observable SN (e.g., a collapsar with a fallback SN, Woosley & Weaver 1995; Iwamoto et al. 2005; Moriya et al. 2010). However, it should be noted that the metallicity of GRB host galaxies may be systematically different from that of direct environments of GRBs (Niino 2011).

Tominaga et al. (2007) suggested that GRBs associated with hypernovae and GRBs without SN features belong to a continuous population, predicting the existence of GRBs associated with sub-luminous or faint SNe with a ^{56}Ni mass of $\sim 10^{-3}$–$10^{-1}\,M_\odot$. The limit on the SN associated with GRB 100418A based on the noise spectrum corresponds to 15% of the luminosity of SN 1998bw at the peak of its light curve (figure 5). Assuming that the mass of ^{56}Ni in SN ejecta is proportional to the luminosity of the SN, the mass of ^{56}Ni ejected from GRB 100418A is $\lesssim 10^{-1}\,M_\odot$ (the ^{56}Ni mass ejected from GRB 980425/SN 1998bw is $\sim 0.5\,M_\odot$, Iwamoto et al. 1998; Nomoto et al. 2001). In jet-induced hypernova models by Tominaga et al. (2007), the ejected amount of ^{56}Ni is smaller if the jet formation is slower, so that the ram pressure of the jet is lower.

If long GRBs without an observable SNe occur from non-collapsar origin, many of the long GRBs that occur in high-metallicity galaxy may be non-collapsar GRBs. In the five GRBs whose host galaxies have spectroscopically measured metallicity $12 + \log({\rm O/H}) > 8.6$ at $z < 1.0$, two are without an SN component to a significant limit, and the other three don't have a confirmed SN component. Considering the claimed low-metallicity preference of the collapsar model (Yoon & Langer 2005; Woosley & Heger 2006; see, however, Fryer et al. 2007), these observations suggests that significant contamination of non-collapsar originates events [e.g., GRBs originates in merger of double compact object binary, so-called short GRBs or Type I GRBs (Zhang et al. 2009)] in the sample of $T_{90} > 2$ s GRBs in high-metallicity galaxies, and possibly also those events in low-metallicity galaxies.

We thank A. de Ugarte Postigo, G. Leloudas, and T. Sakamoto for helpful discussions. Thanks are also due to our referee whose helpful advice largely improved this paper. YN is supported by the Grant-in-Aid for JSPS Fellows.

References

Amati, L. 2006, MNRAS, 372, 233
Amati, L., Della Valle, M., Frontera, F., Malesani, D., Guidorzi, C., Montanari, E., & Pian, E. 2007, A&A, 463, 913
Antonelli, L. A., et al. 2010, GCN Circ., 10620
Baldry, I. K., & Glazebrook, K. 2003, ApJ, 593, 258
Berger, E. 2009, ApJ, 690, 231
Bikmaev, I., et al. 2010a, GCN Circ., 10700
Bikmaev, I., et al. 2010b, GCN Circ., 10726

Bruzual, G., & Charlot, S. 2003, MNRAS, 344, 1000
Caito, L., Bernardini, M. G., Bianco, C. L., Dainotti, M. G., Guida, R., & Ruffini, R. 2009, A&A, 498, 501
Calzetti, D., Armus, L., Bohlin, R. C., Kinney, A. L., Koornneef, J., & Storchi-Bergmann, T. 2000, ApJ, 533, 682
Campana, S., et al. 2011, Nature, 480, 69
Cucchiara, A., & Fox, D. B. 2010, GCN Circ., 10624
Della Valle, M., et al. 2006, Nature, 444, 1050
Drout, M. R., et al. 2011, ApJ, 741, 97
Filgas, R., Klose, S., & Greiner, J. 2010, GCN Circ., 10617
Fryer, C. L., et al. 2007, PASP, 119, 1211
Fynbo, J. P. U., et al. 2006, Nature, 444, 1047
Gal-Yam, A., et al. 2006, Nature, 444, 1053
Galama, T. J., et al. 1998, Nature, 395, 670
Gehrels, N., et al. 2006, Nature, 444, 1044
Holland, S. T., Marshall, F. E., Page, M., de Pasquale M., & Siegel, M. H. 2010, GCN Circ., 10661
Iye, M., et al. 2004, PASJ, 56, 381
Iwamoto, K., et al. 1998, Nature, 395, 672
Iwamoto, N., Umeda, H., Tominaga, N., Nomoto, K., & Maeda, K. 2005, Science, 309, 451
Izotov, Y. I., Stasińska, G., Meynet, G., Guseva, N. G., & Thuan, T. X. 2006, A&A, 448, 955
Kashikawa, N., et al. 2002, PASJ, 54, 819
Kewley, L. J., & Ellison, S. L. 2008, ApJ, 681, 1183
Kobulnicky, H. A., & Kewley, L. J. 2004, ApJ, 617, 240
Levesque, E. M., & Kewley, L. J. 2007, ApJ, 667, L121
Levesque, E. M., Kewley, L. J., Berger, E., & Zahid, H. J. 2010, AJ, 140, 1557
Lu, Y., Huang, Y. F., & Zhang, S. N. 2008, ApJ, 684, 1330
Malesani, D. 2010, GCN Circ., 10621
Marshall, F. E., et al. 2010, GCN Circ., 10612
Marshall, F. E., et al. 2011, ApJ, 727, 132
Marshall, F. E., & Holland, S. T. 2010, GCN Circ., 10720
Mazzali, P. A., et al. 2002, ApJ, 572, L61
McBreen, S., et al. 2008, ApJ, 677, L85
Moriya, T., Sauer, D. N., Mazzali, P. A., Maeda, K., & Suzuki, T. 2010, ApJ, 719, 1445
Nagao, T., Maiolino, R., & Marconi, A. 2006, A&A, 459, 85
Niino, Y. 2011, MNRAS, 417, 567
Nomoto, K., et al. 2001, Supernovae and Gamma-Ray Bursts: the Greatest Explosions since the Big Bang, ed. M. Livio et al. (Cambridge: Cambridge University Press), 144
Ofek, E. O., et al. 2007, ApJ, 662, 1129
Perley, D. A., Cenko, S. B., Miller, A. A., Poznanski, D., Filippenko, A. V., Bloom, J. S., & Nugent, P. 2010, GCN Circ., 10727
Richardson, D. 2009, AJ, 137, 347
Rumyantsev, V., & Pozanenko, A. 2010a, GCN Circ., 10783
Rumyantsev, V., & Pozanenko, A. 2010b, GCN Circ., 10883
Sakamoto, T., et al. 2009, ApJ, 693, 922
Salpeter, E. E. 1955, ApJ, 121, 161
Savaglio, S., et al. 2005, ApJ, 635, 260
Savaglio, S., Glazebrook, K., & Le Borgne, D. 2009, ApJ, 691, 182
Sawicki, M. 2012, PASP submitted
Schlegel, D. J., Finkbeiner, D. P., & Davis, M. 1998, ApJ, 500, 525
Smith, J. A., et al. 2002, AJ, 123, 2121
Soderberg, A. M., et al. 2007, ApJ, 661, 982
Stetson, P. B. 2000, PASP, 112, 925
Thöne, C. C., et al. 2008, ApJ, 676, 1151
Thöne, C. C., et al. 2011, Nature, 480, 72
Tominaga, N., Maeda, K., Umeda, H., Nomoto, K., Tanaka, M., Iwamoto, N., Suzuki, T., & Mazzali, P. A. 2007, ApJ, 657, L77
Tremonti, C. A., et al. 2004, ApJ, 613, 898
Volnova, A., Ibrahimov, M., Karimov, R., & Pozanenko, A. 2010, GCN Circ., 10821
Woosley, S. E., & Heger, A. 2006, ApJ, 637, 914
Woosley, S. E., & Weaver, T. A. 1995, ApJS, 101, 181
Xu, D., et al. 2009, ApJ, 696, 971
Yabe, K., Ohta, K., Iwata, I., Sawicki, M., Tamura, N., Akiyama, M., & Aoki, K. 2009, ApJ, 693, 507
Yoon, S.-C., & Langer, N. 2005, A&A, 443, 643
Zhang, B., et al. 2009, ApJ, 703, 1696